Characterisation of the high-pressure structural transition and elastic properties in boron arsenic*

Lü Bing(吕 兵)[a)b)], Linghu Rong-Feng(令狐荣锋)[a)b)], Yi Yong(易 勇)[c)], and Yang Xiang-Dong(杨向东)[a)†]

[a)] *Institute of Atomic and Molecular Physics, Sichuan University, Chengdu* 610065, *China*
[b)] *School of Physics and Electronic Science, Guizhou Normal University, Guiyang* 550001, *China*
[c)] *School of Materials Science and Engineering, Southwest University of Science and Technology, Mianyang* 621900, *China*

(Received 14 October 2009; revised manuscript received 19 December 2009)

This paper carries out the First principles calculation of the crystal structures (zinc blende (B3) and rocksalt (B1)) and phase transition of boron arsenic (BAs) based on the density-functional theory. Using the relation between enthalpy and pressure, it finds that the transition phase from the B3 structural to the B1 structural occurs at the pressure of 113.42GPa. Then the elastic constants C_{11}, C_{12}, C_{44}, bulk modulus, shear modulus, Young modulus, anisotropy factor, Kleinman parameter and Poisson ratio are discussed in detail for two polymorphs of BAs. The results of the structural parameters and elastic properties in B3 structure are in good agreement with the available theoretical and experimental values.

Keywords: phase transition, elastic properties, generalised gradient approximation, boron arsenic
PACC: 6220D, 6220M, 6430

1. Introduction

Boron arsenic (BAs) compound is a kind of wide band gap semiconductor and an attractive material due to its use in optical and high-temperature applications. Apparently its unusual properties are related to the absence of the p electrons in the core and the small core size of the B atom, as shown by several studies.[1−3] The phase transition from the zinc-blende (B3) structure to the rocksalt (B1) structure has attracted much interest of physicists.[3−5] The generally accepted view is that BAs crystallises in the B3 at ambient conditions but at high pressures it transforms first into B1 structure.

Up to now, several research groups have theoretically investigated the pressure induced phase transitions in BAs using different methods. For example, Wentzcovich and Cohen[4] predicted a phase transition from the zinc-blende (B3) to the sixfold coordinated rocksalt (B1) structure at 110 GPa. Full potential linearised augmented plane-wave (FP-LAPW) calculations showed that the B3/B1 coexistence pressure was 93 GPa in BAs.[3] Recently, Cui *et al.*[5] show the structure phase transition at the transition pressure of 134 GPa, however, obvious differences exist between the results of Refs. [3] and [4].

It is well known that the mechanical properties assessment of material can be made by the determination of its elastic constants. Especially, the elastic constants of materials at high pressures are essential in order to predict and understand material response, strength, and so on.[6−10] In recent years, several theoretical methods have been applied successfully to the calculation of elastic constants of BAs, such as the first-principles pseudopotential total energy method based on the density-functional theory (DFT) within the local density approximation (LDA)[11] and the augmented plane-wave plus local-orbitals (APW+LO) method.[12] However, only very few theoretical investigations on elastic properties with the pressures have been reported in the literature.

In this work, the phase transition and elastic properties are investigated in detail for BAs in the B3 and B1 structures. The results obtained are in good agreement with the available experimental data and other theoretical calculation. In Section 2, a brief description of computational method is given. The

*Project supported by the National Natural Science Foundation of China (Grant Nos. 10974139 and 10964002), the Specialized Research Fund for the Doctoral Program of Higher Education of China (Grant No. 20050610010), the Science-Technology Foundation of Guizhou Province of China (Grant Nos. [2009]2066 and [2009]06), the project of Aiding Elites' Research Condition of Guizhou Province of China (Grant No. TZJF-2008-42).
†Corresponding author. E-mail: xdyang@scu.edu.cn
© 2010 Chinese Physical Society and IOP Publishing Ltd

results of structural phase transition and elastic properties are discussed in Section 3. Finally, the summary of our main results and conclusion are given in Section 4.

2. Computational methods

All calculations on BAs are carried out by using first principles based on the DFT. The electronic exchange and correlation functions are treated within DFT via generalised gradient approximation (GGA).[13] Wave functions are expanded by the plane waves up to a cutoff energy of 450 eV for both B3 and B1 structures of BAs. Brillouin-zone integrations are approximated by using the special k-point sampling of Monkhorst–Pack scheme with a 11×11×11 grid. The convergence of the total energy with respect to both k-point sampling and plane-wave cutoff energy is carefully examined. The reference configurations for valence electrons were $2s^2 2p^1$ for B, $4s^2 4p^3$ for As, respectively. Figure 1 shows the crystal structures of BAs in B3 and B1 phases.

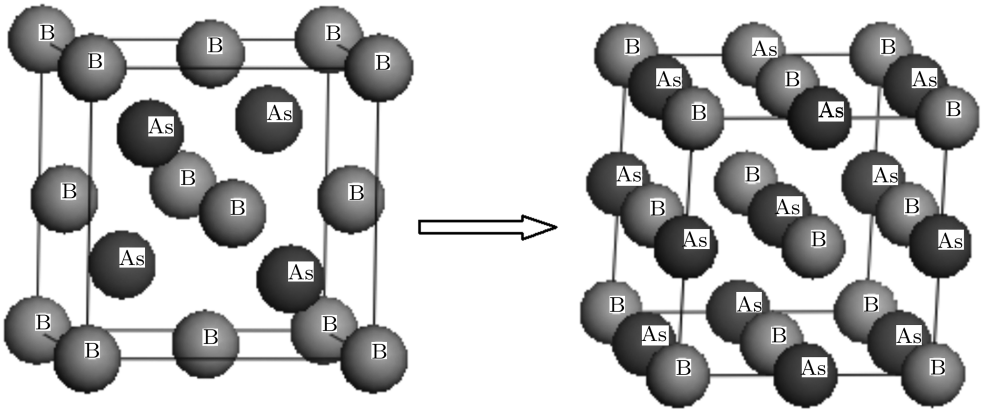


Fig. 1. The two structures of BAs.

2.1. The elastic stiffness constants

The elastic constants of solids provide a link between the mechanical and dynamical behaviour of crystals and give important information concerning the nature of the forces operating in solids. In particular, elastic constants provide information on the stability and stiffness of materials, since the forces and the elastic constants are functions of the first-order and second-order derivatives of the potentials, the calculation of elastic constants will provide a further check on the accuracy of the calculation of forces in solids. For a cubic lattice, there are three independent elastic constants C_{11}, C_{12}, and C_{44}. The elastic constants can be obtained by applying a set of deformation values and calculating the change of energy. First, the lattice parameter is determined at different pressures by using Birch–Murnaghan equation of state. Then the cubic cell with lattice constant is chosen as the reference structure for this pressure and the changes in the total energy are investigated for a set of deformation values. Finally, the Bulk modulus, and the three independent elastic stiffness constants are obtained by 2nd-order function fitting.

To determine the tetragonal Shear modulus $C_{11} - C_{12}$, we considered a volume-conserving tetragonal strain tensor

$$\varepsilon = \begin{pmatrix} \delta & 0 & 0 \\ 0 & -\delta & 0 \\ 0 & 0 & \delta^2/(1-\delta^2) \end{pmatrix}.$$

Here, δ is the deformation parameter. Application of this strain causes an energy change

$$\Delta E(\delta) = (C_{11} - C_{12}) V_0 \delta^2 + O(\delta^4), \qquad (1)$$

where, V_0 is the volume of the unstrained unit cell, $O(\delta^4)$ denotes the higher order items of δ.

For an isotropic cubic crystal, the bulk modulus is given exactly by

$$B = (C_{11} + 2C_{12})/3. \qquad (2)$$

Furthermore we have used the following isotropic

strain tensor to calculate the bulk modulus:

$$\varepsilon = \begin{pmatrix} \delta & 0 & 0 \\ 0 & \delta & 0 \\ 0 & 0 & \delta \end{pmatrix},$$

which yields the deformation energy equation such as

$$\Delta E(\delta) = (9BV_0/2)\delta^2. \tag{3}$$

In terms of Eqs. (1)–(3), the C_{11} and C_{12} can be derived.

For the pure shear elastic constant C_{44}, we have applied the following strain tensor given by

$$\varepsilon = \begin{pmatrix} 0 & \delta/2 & 0 \\ \delta/2 & 0 & 0 \\ 0 & 0 & \delta^2/(4-\delta^2) \end{pmatrix},$$

the energy change associated with this strain is then

$$\Delta E(\delta) = C_{44}V_0\delta^2/2 + O(\delta^4). \tag{4}$$

Bulk modulus or shear modulus can measure the hardness in an indirect way.[14] The shear modulus is given in the following expression; $G = (G_{\rm V} + G_{\rm R})/2$. Here, $G_{\rm R}$ is Reuss modulus given by

$$G_{\rm R} = \frac{5(C_{11} - C_{12})C_{44}}{4C_{44} + 3(C_{11} - C_{12})}, \tag{5}$$

and $G_{\rm V}$ the Voigt modulus defined as

$$G_{\rm V} = (3C_{44} + C_{11} - C_{12})/5. \tag{6}$$

Kleinman parameter is important parameter describing the relative position of the cation and anion sublattices. It is given by the following relation:[15]

$$\xi = \frac{C_{11} + 8C_{12}}{7C_{11} + 2C_{12}}. \tag{7}$$

It is well known that microcracks are induced in crystal owing to the elastic anisotropy and so on. Essentially, all known crystals are elastically anisotropic. A convenient method of describing the degree of elastic anisotropy for a cubic crystal has been defined as[16]

$$A^* = \frac{3(A-1)^2}{[3(A-1)^2 + 25A]}, \tag{8}$$

where $A = 2C_{44}/(C_{11} - C_{12})$ is the usual anisotropy factor. Generally, A^* is zero for elastically isotropic crystal. For an anisotropic crystal, A^* is always positive and a single valued measure of the elastic anisotropy regardless of whether A smaller or larger than 1. Further, it is shown that A^* gives the relative magnitude of the actual elastic anisotropy possessed by the crystal.

The Young modulus E and Poisson ratio γ are then calculated by

$$E = \frac{9BG}{3B + G}, \tag{9}$$

and

$$\gamma = \frac{3B - E}{6B}. \tag{10}$$

3. Results and discussions

Total energy versus volume data for the B1 and B3 phases of BAs are shown in Fig. 2. From Fig. 2, it is obvious that B3 phase is more stable than B1, and then a least-square fitting of these data are made to the 3rd-order Birch–Murnaghan equation of state (EOS) for each phase.

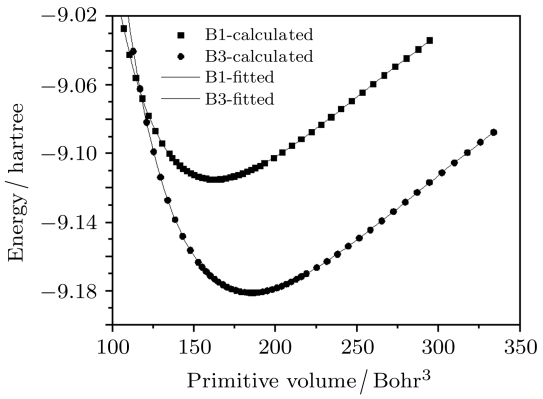


Fig. 2. Energy as a function of primitive cell volume for BAs. (1 hartree = 110.5×10^{-21} J).

In the 3rd-order Birch–Murnaghan EOS, the total energy and pressure as a function of volume are given as:[17]

$$E(V) = E_0 + \frac{9V_0B_0}{16}\left\{\left[\left(\frac{V_0}{V}\right)^{2/3} - 1\right]^3 B' + \left[\left(\frac{V_0}{V}\right)^{2/3} - 1\right]^2 \left[6 - 4\left(\frac{V_0}{V}\right)^{2/3}\right]\right\}, \tag{11}$$

$$P(V) = \frac{3B_0}{2}\left\{\left[\left(\frac{V_0}{V}\right) - \left(\frac{V_0}{V}\right)^{5/3}\right]^{7/3}\right\} \times \left\{1 + \frac{3}{4}(B' - 4)\left[\left(\left(\frac{V_0}{V}\right)^{2/3} - 1\right)\right]\right\}, \tag{12}$$

where, E_0 is the total energy, V_0 is the equilibrium volume, B_0 is the bulk modulus at $P = 0$ GPa, and B' is the first derivative of the bulk modulus with respect to pressure. The calculated structure parameters of BAs are listed in Table 1, together with the experimental data and other theoretical results. The agreement among them is good.

Table 1. The lattice constants a, bulk modulus B_0 and its pressure derivation B'_0 of the B3 and B1 structures of BAs at $P = 0$ and $T = 0$, together with the transition pressures P_t.

	this work	other theoretical calculation	experiments
B3 structure			
a/Å	4.779	4.777[a],4.736[b], 4.741[c],4.784[d]	4.777[e]
B_0/GPa	138.285	145[a],137[b],147.5[c],145[d]	
B'_0	4.086	3.49[b],4.216[c],3.78[d]	
P_t	113.42	110[a],134[b],93[d]	
B1 structure			
a/Å	4.581	4.583[a],4.546[b], 4.619[d]	
B_0/GPa	142.884	143[a],147[b],135[d]	
B'_0	3.825	3.73[b],3.44[d]	

[a] From Ref. [4]; [b] From Ref. [5]; [c] From Ref. [17]; [d] From Ref. [3]; [e] From Ref. [18]. (1 Å = 0.1 nm)

To find out the transition pressure, Gibbs free energy relation $G = E + PV - TS$ is applied. Being the phase transition pressure independent of the temperature, last term is ignored, and corresponding relation for Gibbs free energy reduces to enthalpy relation $H = E + PV$. In order to find out transition pressure from B3 structure to B1, a common tangent is drawn to the B3 and the B1 energy curves. By measuring the slope of this tangent theoretical transition pressure is obtained (transition pressure is that pressure where the enthalpy parameter for both structures become equal). The enthalpy obtained, H, as a function of pressure P, is illustrated in Fig. 3. The changeover from B3 to B1 occurs around 113.42 GPa which is in good agreement with the theoretical values 110 GPa, 93 GPa reported in Ref. [3] and [4].

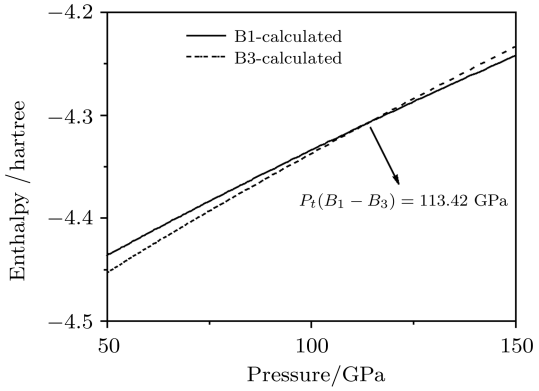


Fig. 3. Enthalpy as a function of pressure for BAs.

For the transition pressure of 113.42 GPa, we illustrate the normalised primitive cell volume V/V_0 (V_0 is the zero-pressure equilibrium primitive cell volume) dependences on pressure P at $T = 0$, 1000 K in Fig. 4. Obviously, when temperature increases, the curve of $V/V_0 - P$ becomes steeper, indicating that BAs is compressed much more easily at higher temperature. For both the B3 structure and B1 structure of BAs at $T = 0$ K, the results are close to the theoretical results of Cui *et al.*[5]

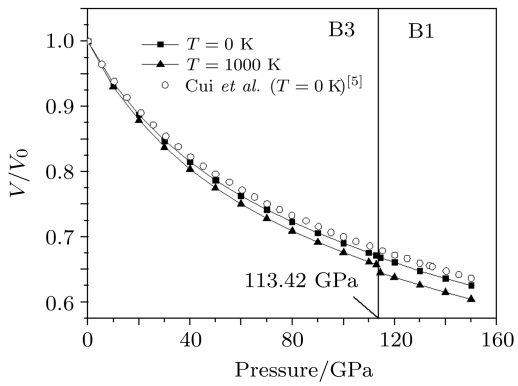


Fig. 4. The normalised volume-pressure diagram of B3 and B1 structures for BAs at various temperatures.

Figure 5 shows the elastic constants (C_{11}, C_{12} and C_{44}) at the different pressures for both B3 and B1 structures. From these curves, one can see that all the calculated elastic constants are everywhere positive and increase monotonically with the pressure except for C_{44} which slowly decreases in the B1 structure. In Table 2, we present the elastic constants of two structures under high pressure, in comparison with the theoretical work of Herrera-Cbrera *et al.*[11]

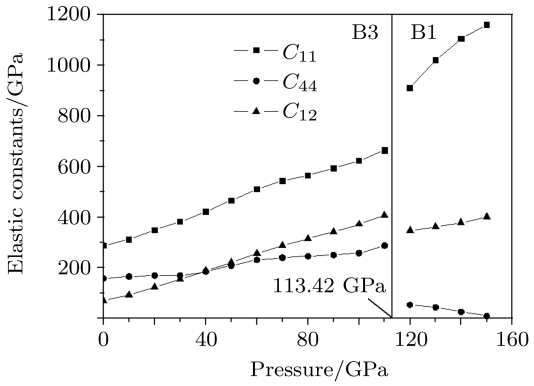


Fig. 5. The elastic constants versus pressure for BAs.

For a cubic crystal, the mechanical stability under isotropic pressure can be judged from the following condition:[19]

$$\tilde{C}_{44} > 0, \quad \tilde{C}_{11} > \left|\tilde{C}_{12}\right|, \quad \tilde{C}_{11} + 2\tilde{C}_{12} > 0. \tag{13}$$

Where $\tilde{C}_{ii} = C_{ii} - P(ii = 1, 4)$, $\tilde{C}_{22} = C_{22} + P$. When $P > 120$ GPa, we find that $\tilde{C}_{11} < \left|\tilde{C}_{12}\right|$ for the B3 structure BAs, and the elastic constants $\tilde{C}_{ij}$ of the B1 structure BAs are consistent with Eq. (13), indicating that when $P > 120$ GPa, the B3 structure BAs is unstable, and the B1 structure BAs is stable. Therefore, we judge from the high pressure elastic constants that the phase transition of BAs from B3 to B1 should occur at a pressure below 120 GPa, consistent with the phase transition pressure 113.42 GPa obtained from equal enthalpies.

Table 2. Calculated elastic constants C_{11}, C_{44} and C_{12}, bulk modulus B, shear modulus G, Young modulus E, Kleinman parameter ξ, degree of elastic anisotropy A^* and Poisson ratio γ for B3 structure at various pressures P.

P/GPa	C_{11}/GPa	C_{12}/GPa	C_{44}/GPa	B/GPa	G/GPa	E/GPa	B/G	A	ξ	A^*	γ
This work											
0	286.388	70.963	157.503	142.772	135.256	308.384	1.055	1.462	0.398	0.017	0.14
10	312.175	92.213	164.890	165.534	140.184	327.971	1.181	1.499	0.443	0.019	0.169
20	348.764	122.47	169.912	197.9	144.36	348.373	1.371	1.501	0.494	0.02	0.206
50	466.55	222.1	209.017	303.583	168.541	426.665	1.801	1.71	0.604	0.034	0.265
100	622.722	371.7	258.208	461.373	193.566	509.454	2.383	2.191	0.716	0.072	0.316
110	663.244	407.33	287.497	502.635	202.802	536.279	2.478	2.386	0.736	0.088	0.322
120	690.05	461.07	302.771	537.399	205.047	545.732	2.621	2.644	0.761	0.109	0.331
140	766.07	508.91	312.071	603.298	214.206	574.612	2.816	2.556	0.771	0.102	0.341
Herrera-Cbrera *et al.*[11]											
0	301.4	78.557	165.13	150.7							
10	346.39	113.93	186.07	192.49							
20	388.12	149.3	200.6	226.25							
50	495.89	242.58	234.57	327.55							
100	651.9	396.99	270.34	481.96							
110	679.26	427.56	275.25	512.53							
120	696.22	459.72	280.16	541.48							
140	762.92	517.63	288.38	597.79							

Table 3. Calculated elastic constants C_{11}, C_{12} and C_{44}, bulk modulus B, shear modulus G, Young modulus E, Kleinman parameter ξ, degree of elastic anisotropy A^* and Poisson ratio γ for B1 structure at various pressures P.

P/GPa	C_{11}/GPa	C_{12}/GPa	C_{44}/GPa	B/GPa	G/GPa	E/GPa	B/G	A	ξ	A^*	γ
This work											
0	190.445	107.814	65.061	135.358	54.231	143.526	2.495	1.574	0.679	0.024	0.323
20	296.001	152.459	52.099	200.307	59.241	161.776	3.381	0.726	0.637	0.012	0.365
50	423.856	243.643	47.533	303.714	61.586	173.062	4.931	0.527	0.687	0.048	0.405
100	764.747	310.024	52.515	461.599	99.149	277.575	4.655	0.231	0.543	0.235	0.399
110	830.036	328.606	58.044	495.749	109.46	305.866	4.529	0.231	0.535	0.234	0.397
120	910.072	346.443	53.558	534.319	122.34	341.21	4.768	0.19	0.521	0.293	0.402
130	1019.67	361.453	43.811	580.859	112.49	317.027	5.163	0.133	0.497	0.404	0.409
140	1105.07	377.979	26.427	620.343	101.64	289.136	6.103	0.072	0.486	0.586	0.422

The bulk modulus (B), shear modulus (G), Young modulus (E), Kleinman parameter (ξ), degree of elastic anisotropy (A^*) and Poisson ratio (γ) of the B3 and B1 structures at the different pressures are listed in Tables 2 and 3, respectively. As no experimental and theoretical data are available for both structures, therefore, the results can serve as a basis for future experimental and theoretical investigations. The Young's modulus E is defined as the ratio between stress and strain, and is used to provide a measure of the stiffness of the solid, i.e., the larger the value of E, the stiffer is the material. It is clear that B3 structure has a larger stiffness than B1 structure, and B3 structure is hard to be broken because the E is higher than B. Pugh[20] introduced the quotient of bulk to shear modulus (B/G) of polycrystalline phases by considering that the shear modulus G represents the resistance to plastic deformation, while the bulk modulus B represents the resistance to fracture. A high (low) B/G value is associated with ductility (brittleness). The critical value which separates ductile and brittle materials is about 1.75. All the calculated values of the B/G (> 1.75) increase with pressures which means that pressure can improve ductility. The plots of B, G and E for the B3 and B1 structures as a function of pressure are depicted in Fig. 6. It is noted from Fig. 6 that the pressure has an important influence on the B, G and E. Despite of some fluctuations in the E and G values for B3 structure, the general linear dependence trend on the pressure is observed.

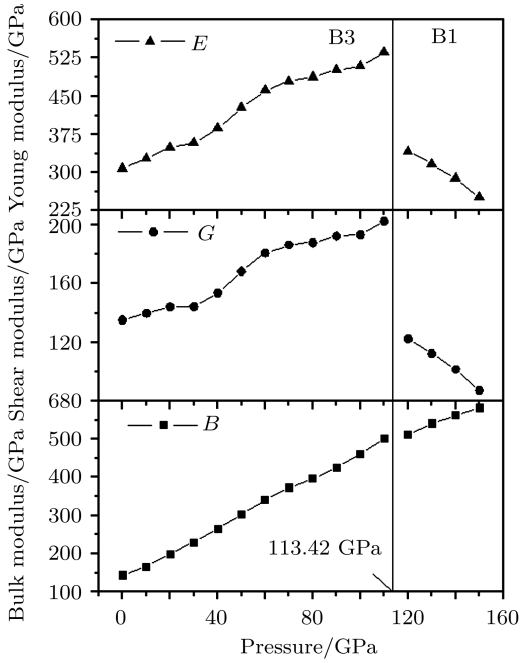


Fig. 6. Bulk, shear and Young modulus for B3 and B1 structures as a function of pressure.

The Poisson's ratio γ provides more information about the characteristics of the bonding forces than any of the other elastic constants. The $\gamma = 0.25$ and 0.5 are the lower limit and upper limit for central force solids, respectively. In our case, γ increases with applied pressure in Tables 2 and 3, and the interatomic forces in the BAs are predominantly central forces. The elastic anisotropy of crystals has an important implication in engineering science since it is highly correlated with the possibility to induce microcracks in the materials. Therefore, the anisotropy factor $A = 2C_{44}/(C_{11} - C_{12})$ has been evaluated to provide insight on the elastic anisotropy of the BAs. In the wide range of applied pressure, the obtained anisotropy factors A are not equal to 1. This shows the elastic anisotropy in BAs. Figure 7 displays the variation of the Kleinman parameter (ξ), the degree of elastic anisotropy (A^*) and the Poisson's ratio (γ) of B3 and B1 structures at different pressures. It is clear that ξ, A^* and γ increase with increasing pressure in B3 and B1 structures, while in B1 structure, ξ decreases slightly with increasing pressure. From Fig. 7, we can also find that the degree of elastic

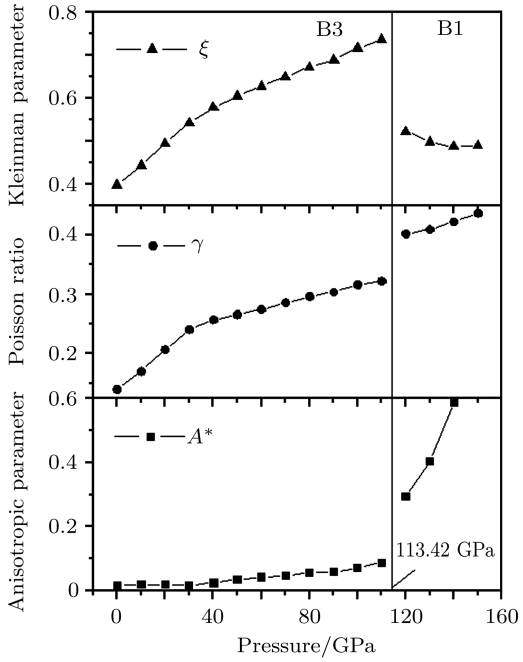


Fig. 7. Kleinman parameter, degree of elastic anisotropy and Poisson ratio for B3 and B1 structures as a function of pressure.

anisotropy A^* in BAs increases as the pressure increases and tends to a linear increase, and B1 structure increases markedly in comparison with B3 structure. It can be seen from Tables 2 and 3 that BAs crystal

is characterised by a profound elastic anisotropy since the anisotropy factor $A^* < 1$ for both B3 structure and B1 structure, and the degree of elastic anisotropy for B3 structure is smaller than B1 structure of the BAs.

4. Conclusions

In summary, the phase transition and elastic properties of BAs have been investigated based on DFT. The pressure of transition is 113.42 GPa from the equal enthalpies, which is consistent with the other theoretical data.[3,4] The elastic properties are discussed in detail for BAs in the B3 and B1 structures. The obtained high pressure elastic constants indicated a close agreement with the reported literature data.[11] In addition, other calculated parameters such as shear modulus, Young modulus, Kleinman parameter, anisotropy parameter and Poisson ratio are also presented in this work.

References

[1] Bouhafs B, Aourag H and Certier M 2000 *J. Phys.*: *Condens. Mat.* **12** 5655

[2] Lambrecht W R L and Segall B 1991 *Phys. Rev.* B **43** 7070

[3] Zaoui A and Hassan F 2001 *J. Phys.*: *Condens. Mat.* **13** 253

[4] Wentzcovitch R M and Cohen M L 1987 *Phys. Rev.* B **36** 6058

[5] Cui S X, Feng W X, Feng Z and Wang Y 2009 *Comput. Mater. Sci.* **44** 1386

[6] Liu N N, Song R B and Du D W 2009 *Chin. Phys.* B **18** 1979

[7] Wang C L, Yu B H, Huo H L, Chen D and Sun H B 2009 *Chin. Phys.* B **18** 1248

[8] Zhu J, Yu J X, Wang Y J, Chen X R and Jing F Q 2008 *Chin. Phys.* B **17** 2216

[9] Hao Y J, Cheng Y, Wang Y J and Chen X R 2007 *Chin. Phys.* **16** 217

[10] Liu Z J, Qi J H, Guo Y, Chen Q F, Cai L C and Yang X D 2007 *Chin. Phys.* **16** 499

[11] Herrera-Cabrera M J, Rodríguez-Hernández P and Muñoz A 2003 *Int. J. Quantum Chem.* **91** 191

[12] Meradji H, Drablia S, Ghemid S, Belkhir H, Bouhafs B and Tadjer A 2004 *Phys. Stat. Sol.* B **241** 2881

[13] Perdew J P, Burke K and Ernzerhof M 1996 *Phys. Rev. Lett.* **77** 3865

[14] Monkhorst H J and Pack J D 1976 *Phys. Rev.* B **13** 5188

[15] Teter D M 1998 *MRS Bull.* **23** 22

[16] Chung D H and Buessem W R 1967 *J. Appl. Phys.* **38** 2010

[17] Shimizu H and Sasaki S 1992 *Science* **257** 514

[18] Ahmed R, Hashemifar S J, Akbarzadeh H and Ahmed M 2007 *Comput. Mater. Sci.* **39** 580

[19] Sin'ko G V and Smirnow N A 2002 *J. Phys. Condens. Mat.* **14** 6989

[20] Pugh S F 1954 *Phil. Mag.* **45** 823